This paper is available on line at http://www.mcponline.org

A Proteomic Focus on the Alterations Occurring at the Human Atherosclerotic Coronary Intima*[S]

Fernando de la Cuesta‡, Gloria Alvarez-Llamas‡, Aroa S. Maroto‡, Alicia Donado§, Irene Zubiri‡, Maria Posada‡, Luis R. Padial¶, Angel G. Pinto§, Maria G. Barderas‖§§, and Fernando Vivanco‡‡‡§§**

Coronary atherosclerosis still represents the major cause of mortality in western societies. Initiation of atherosclerosis occurs within the intima, where major histological and molecular changes are produced during pathogenesis. So far, proteomic analysis of the atherome plaque has been mainly tackled by the analysis of the entire tissue, which may be a challenging approach because of the great complexity of this sample in terms of layers and cell type composition. Based on this, we aimed to study the intimal proteome from the human atherosclerotic coronary artery. For this purpose, we analyzed the intimal layer from human atherosclerotic coronaries, which were isolated by laser microdissection, and compared with those from preatherosclerotic coronary and radial arteries, using a two-dimensional Differential-In-Gel-Electrophoresis (DIGE) approach. Results have pointed out 13 proteins to be altered (seven up-regulated and six down-regulated), which are implicated in the migrative capacity of vascular smooth muscle cells, extracellular matrix composition, coagulation, apoptosis, heat shock response, and intraplaque hemorrhage deposition. Among these, three proteins (annexin 4, myosin regulatory light 2, smooth muscle isoform, and ferritin light chain) constitute novel atherosclerotic coronary intima proteins, because they were not previously identified at this human coronary layer. For this reason, these novel proteins were validated by immunohistochemistry, together with hemoglobin and vimentin, in an independent cohort of arteries. ***Molecular & Cellular Proteomics 10: 10.1074/mcp.M110.003517, 1–13, 2011.***

Coronary heart disease remains the major cause of mortality in developed countries. In particular, coronary atherosclerosis is the responsible for the majority of the acute coronary syndromes. In the recent years, the understanding of atherosclerosis has experienced a drastic shift, because advances in basic research have pointed out the role of inflammation and the underlying cellular and molecular mechanisms that contribute to atherogenesis (1, 2). Intimal thickening produced by the migration of vascular smooth muscle cells (VSMCs)[1] to the subendothelium, where they synthesize extracellular matrix (ECM), appears during normal development and aging (3), in response to minimal endothelium injury often produced by a disturbance in the pattern of blood flow at bending points and near bifurcations of the arterial tree (4). Atherosclerosis initiates at this locations with circulating leukocytes recruitment because of vascular endothelium alteration, which triggers the expression of adhesion molecules (VCAM) (3). Monocytes differentiate into macrophages within the arterial intima where they phagocyte lipids, finally turning into foam cells (5). Lipid accumulation within the intima leads to the formation of a central lipid core that is surrounded by a fibrous cap generated by migrated VSMCs (6).

Proteomic analysis of plasma, circulating cells or atherome plaque from patients affected by atherosclerosis has lead to a better understanding of the initiation and development of this pathology, because proteins are the final effectors of all events triggered by lipid deposition onto the thickened intima.

Although arterial tissue protein extracts have allowed characterizing many proteins involved in the pathogenesis of atherosclerosis (7), these studies have the limitation of measuring protein levels in all artery locations as a whole. Therefore, proteomic analysis of regions of interest isolated by laser microdisection (LMD) potentially gives more specific results.

From the ‡Department of Immunology, IIS-Fundacion Jimenez Diaz, Madrid, Spain, §Cardiac Surgery Unit, Hospital Gregorio Marañon, Madrid, Spain, ¶Department of Cardiology, Hospital Virgen de la Salud, Toledo, Spain, ‖Department of Vascular Physiopathology, Hospital Nacional de Paraplejicos, SESCAM, Toledo, Spain, **Department of Biochemistry and Molecular Biology I, Universidad Complutense, Madrid, Spain

Received July 23, 2010, and in revised form, December 28, 2010

Published, MCP Papers in Press, January 19, 2011, DOI 10.1074/mcp.M110.003517

[1] The abbreviations used are: VSMC, vascular smooth muscle cell; 2-DE, two-dimensional electrophoresis; ACB, atherosclerotic coronary biopsy; ANXA4, annexin A4; CAN, atherosclerotic coronary necropsy; EC, endothelial cell; ECM, extracellular matrix; FLC, ferritin light chain; H&E, hemtoxilin/eosin staining; IHC, immunohistochemistry; LMD, laser microdissection; LMPC, laser microdissection and pressure catapulting; MFAP4, microfibril-associated glycoprotein 4; MRLC, myosin regulatory light 2, smooth muscle isoform; OGN, osteoglycin; PCN, preatherosclerotic coronary necropsy; PRB, preatherosclerotic radial biopsy; SaP, serum amyloid protein.

One limitation of this technique is that it may require long LMD times to recover sufficient amounts of protein. However, this limitation has been overcome by the combination of LMD with saturation labeling DIGE, a technique based on fluorescent labeling of proteins in Cys residues, which allows analyzing scarce samples by two-dimensional electrophoresis (2-DE) using less than 5 μg of total protein (8).

In many cases, victims of acute coronary syndromes (ACS) do not present prior symptoms. For this reason, there is still need to develop novel early diagnosis biomarkers that could predict future cardiac events in asymptomatic patients. Because atherosclerosis initiates within the intima, we aimed to study atherosclerotic coronary intima proteome compared with nonatherosclerotic intima in the search for potential biomarkers of the disease right at the location where their expression levels start to increase/decrease. On the one hand, their discovery will lead to further understand the pathology and, as they may be finally released into plasma, they may constitute potential targets in early diagnosis, prognosis, or therapy. For this purpose, intima from human atherosclerotic coronary arteries and from preatherosclerotic coronaries and radial arteries was isolated by LMD. A differential abundance analysis was performed by saturation labeling DIGE resulting in the identification by MS of 13 proteins altered, 7 up-regulated and 6 down-regulated. Altered expression of a subset of these proteins was validated by immunohistochemistry (IHC) on an independent group of patients. A schematic view of the workflow of the study performed can be observed in Fig. 1.

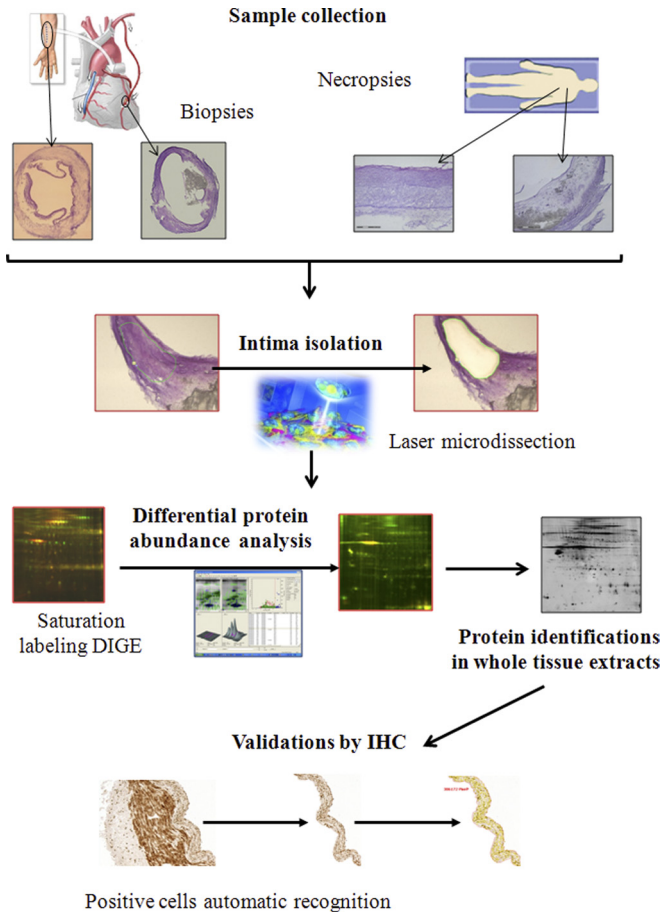

FIG. 1. **Workflow of the differential protein abundance analysis of atherosclerotic coronary intima.** A schematic view of the workflow from the study of atherosclerotic coronary intima differential proteome can be observed in this figure.

EXPERIMENTAL PROCEDURES

Materials—Urea, SDS, Tris, 3-[(3-cholamidopropyl)dimethylammonio]-1-propanesulfonic acid (CHAPS), TBP, and dithiotreitol were purchased from BioRad. Thiourea, ammonium bicarbonate, formic acid (99.5% purity), trifluoroacetic acid, α-cyano-4-hydroxycinnamic acid, acetonitrile, methanol, and protease inhibitor mixture were from Sigma-Aldrich and porcine trypsin from Promega. Cresyl violet (Certistain) was from Merck, TCEP and Protein Desalting Spin Columns from Pierce, and Optimal Cutting Temperature compound (OCT) from Sakura Finitek (Torrence, CA). Polyethylene naphthalate membranes and adhesive cap 500 μl opaque tubes were from PALM Microlaser, Carl Zeiss MicroImaging GmbH, Jena, Germany. CyeDye Fluor Labeling Kit for Scarce Samples, Pharmalyte pH 3–10, and IPG strips (18, pH 4–7) were from GE Healthcare. Mouse antihuman primary antibodies for α-actin and CD68 immunostaining were from Dako. Primary antibodies used for validation by IHC were: annexin A4, ferritin light chain, myosin regulatory light chain, hsp27, phospho-hsp27 (S82 and S78) from Abcam (Cambridge, MA), hemoglobin β from Santa Cruz (Santa Cruz, CA), and vimentin from Serotec (Raleigh, NC). Secondary antibody used for these IHCs was EnVision Dual Link System-HRP, which reacts with both mouse and rabbit hosted primary antibodies.

Human Artery Samples—Human arteries (n = 24. 12 for two-dimensional DIGE and 12 for IHC validation) were from biopsy and necropsy origin. Biopsies from coronary and radial arteries came from patients subjected to coronary bypass surgery at the Gregorio Marañón Hospital in Madrid, Spain, and from heart transplant surgery at the Hospital de la Fe, Valencia, Spain. Coronary necropsies were collected in a timeframe of 4–10 h at the Hospital Virgen de la Salud in Toledo, Spain. Procedures of sample collection applied in each participant institution were approved by the correspondent local ethics committee. Samples were immediately washed in saline, embedded in OCT, frozen with liquid nitrogen and stored at −80 °C until used. In particular, two fragments of two of the arteries used in the DIGE study, an atherosclerotic coronary necropsy and a radial biopsy, were directly frozen in liquid nitrogen and used to obtain a whole tissue extract for MS/MS protein identification, as detailed below.

Histological Characterization and Grouping of Artery Specimens—Consecutive 5-μm sections to those used for LMD were subjected to Hematoxilin-Eosin (H&E) staining and IHC to localize macrophages/foam cells and VSMCs using antibodies against CD68 and actin, respectively (Fig. 2). To create the groups of study, characterization of plaque lesions was performed according to the variation of the American Heart Association (AHA) classification described by Virmani *et al.* (5). Pathological samples were coronary lesions from biopsies (ACB) and necropsies (ACN) assigned as fibrous cap atheromas, which show a well formed lipid core, presence of an inflammatory infiltrate, and evidence of sporadic calcification. Nonatherosclerotic coronary necropsies and radial biopsies selected for the study were those classified as preatherosclerotic.

Control arteries from necropsy origin (PCN) were obtained from individuals who did not die from cardiovascular events and with no evidences of atherosclerotic lesions in any of the most frequently affected arteries. Control coronaries did not present apparent lesions

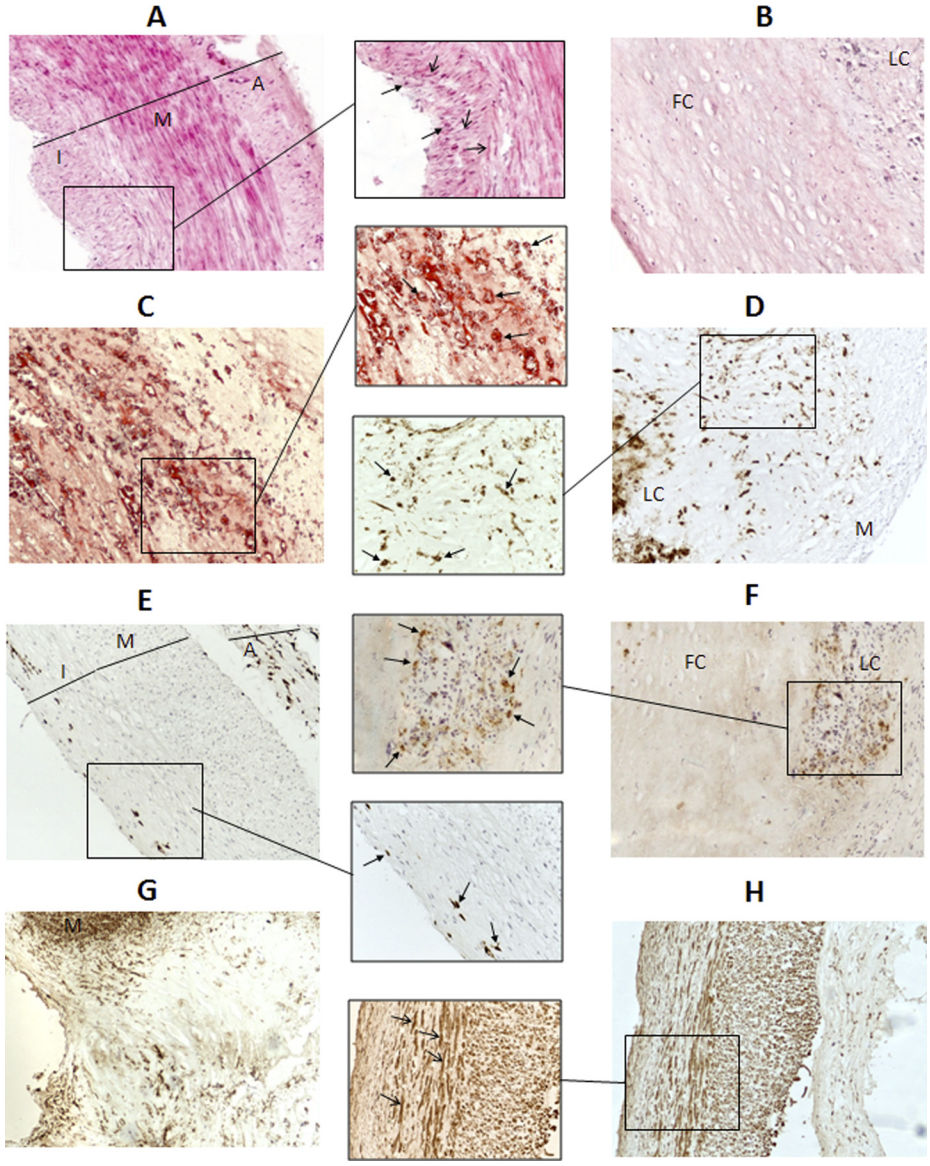

FIG. 2. **Histology of atherosclerotic and preatherosclerotic arteries.** H&E and Oil Red staining, together with CD68 and actin IHC were performed with every artery studied in order to identify the artery architecture and to characterize their atherosclerotic lesion degree. Representative images (100× magnification) of a subset of these analyses can be seen in the figure: *A*, preatherosclerotic radial biopsy, H&E. *B*, atherosclerotic coronary necropsy, H&E. *C*, atherosclerotic coronary necropsy, Oil Red. *D*, atherosclerotic coronary biopsy, CD68. *E*, preatherosclerotic coronary necropsy, CD68. *F*, atherosclerotic coronary necropsy, CD68. *G*, atherosclerotic coronary biopsy, actin. *H*, preatherosclerotic coronary necropsy, actin. In some images, a subregion has been augmented (200× magnification). I: intima. M: media. A: adventitia. LC: lipid core. FB: fibrous cap. *Open-end arrow*: VSMCs. *Closed-end arrow*: macrophages/foam cells.

at macroscopic observation and, at a histologic level, they were classified as preatherosclerotic as they showed an incipient intimal thickening with moderate or absent macrophage infiltration (5). Preatherosclerotic radial arteries (PRB), obtained during bypass surgery, were selected as biopsy control arteries because of the impossibility to obtain nonpathological coronary tissue from biopsy origin.

In addition, histological analysis facilitated intima layer recognition and isolation by LMD.

Preparation of Histological Sections for Laser Microdissection—Sample preparation for laser microdissection has been previously described in detail (9). Briefly, serial 10-μm sections from OCT embedded arteries were cut and placed on Polyethylene naphthalate membrane slides. Tissue sections were fixed with −20 °C precooled 70% ethanol. Following this, a fast staining method with cresyl violet dissolved in ethanol was performed on ice and with all solutions precooled (4 °C) to minimize proteases action. Partially or totally aqueous staining solutions were supplemented with 0.01% protease inhibitor mixture, including fixation 70% ethanol. Slides were placed on ice until LMPC was carried out. Slides were not covered with coverslips as it would impede tissue microdissection.

Isolation of Intima Layer by LMD—Intima layer from arteries addressed to DIGE analysis ($n = 12$) was isolated by LMPC technology (Fig. 3) in a MicroBeam system (PALM Microlaser, Carl Zeiss). For this purpose, the 10× objective was used, applying in most cases an energy rating of 75% for cutting, and 100% for tissue catapulting. Although performing microdissection of initial areas of interest in each artery, the laser conditions were checked and slightly modified when necessary. Selected elements for LMPC were cut and catapulted using the Robo LPC function with microdissection system software (PALM Robo Software 3.2, Carl Zeiss), which allows both cutting and catapulting in a single step. Following LMPC of all areas, each element was checked, and those regions that were not efficiently catapulted were collected by using a single laser pressure-catapulting step with LPC function. In each case, 8 mm^2 of intimal tissue was microdissected and catapulted to a 500 μl adhesive cap tube, because previous studies demonstrated that 4 mm^2 was an adequate amount for saturation labeling DIGE analysis (9) and half of the sample was needed to generate the DIGE pool. Maximum time of microdissection did not exceed in any case 2 h, in order to avoid possible protein degradation. Proteins from isolated tissue were extracted in

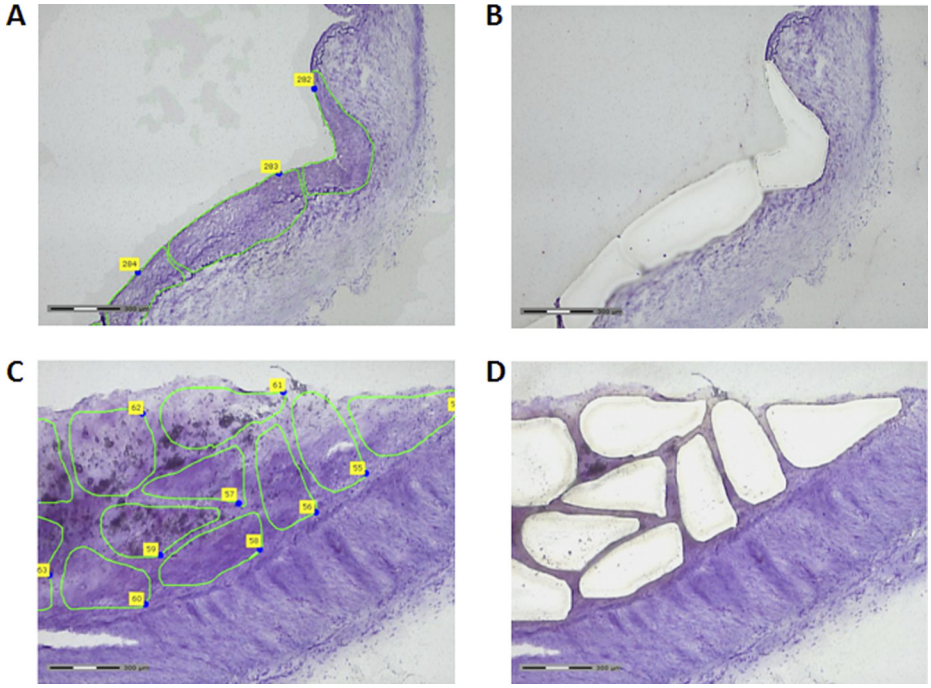

FIG. 3. **Intima layer isolation by LMPC.** An area of 8 mm^2 was isolated by LMPC from the intima layer of all studied arteries for subsequent proteomic analysis. Representative images of a preatherosclerotic radial biopsy with some delimited elements for LMPC (*A*) and with the correspondent cut regions following microdissection (*B*), are shown. Similar images from an atherosclerotic coronary necropsy are also represented (*C*, *D*).

DIGE conventional lysis buffer with the addition of dithiotreitol, as described elsewhere (9).

Saturation Labeling DIGE—The four groups studied by two-dimensional-DIGE were ACB and ACN as pathological samples, and PRB and PCN as control ones. In previous studies (9), a cleaning step performed with Protein Desalting Spin Columns yielded much better two-dimensional DIGE results, and so it was applied prior to the acetone precipitation step needed to obtain the sample volume recommended for an efficient DIGE labeling. Previous to the labeling, samples were reduced with 1 nmol Tris 2-carboxyethyl phosphine at 37 °C for 1 h in the dark. Half of each sample of the study was added to a pool to be used as internal standard in all gels for the two-dimensional DIGE analysis. Samples were labeled with 2 nmol of Cy5 dye and the pool with an equivalent amount of Cy3, at 37 °C for 30 min in the dark.

Two-dimensional Gel Electrophoresis—Each Cy5-labeled sample was mixed with an equal amount of Cy3-labeled pool and loaded on 18 cm, pH 4–7, IPG strips, by anodic cup-loading. IEF was performed on PROTEAN IEF Cell (BioRad) as previously described (9). Second dimension was performed on 12.5% polyacrylamide gels using the EttanDalt Six System (GE Healthcare).

Differential Abundance Protein Analysis and PCA Analysis—2-DE gels were scanned at a resolution of 100 ppm in a Typhoon 9400 scanner (GE Healthcare). Images were imported to DeCyder software (GE Healthcare) where spot detection and matching is performed with the internal standard loaded on each gel. Differential abundance analysis of matched spots was performed by Student's t-Test analysis of the following comparisons: pathological *versus* control from the same origin (ACB *versus* PRB, ACN *versus* PCN), pathological *versus* control from different origin (ACB *versus* PCN, ACN *versus* PRB) and control samples from different origin (PCN *versus* PRB). Spots found significantly varied (p *value* $\leq$ 0.05) and with a fold change greater than 2.0 or lower than −2.0 were considered for further analysis. In addition, principal components analysis (PCA) was performed with Extended Data Analysis module from DeCyder, in order to secure adequate grouping of the arteries. Forty-one spots selected for this statistical analysis were those found significantly varied in an Anova Test performed with the four groups under study (p *value* $\leq$ 0,05).

Preparative Two-dimensional DIGE Gels—Because microdissected material collected was insufficient to run preparative gels to perform protein identifications, whole artery tissue extracts from two of the arteries used in the DIGE experiment were obtained. Proteins were extracted in lysis buffer containing 7 M urea, 2 M thiourea, 30 mM Tris, and 4% CHAPS after having crushed the frozen tissue with a mortar. Extracts were subsequently sonicated for 15 min and tissue debris were removed by centrifugation at 12000 × *g*. Supernatant was stored at −80 °C until use. An amount of 300 μg of total protein was reduced with 60 nmol Tris 2-carboxyethyl phosphine and labeled with 120 nmol preparative Cy3 dye. Following labeling, tissue extracts were loaded on 18-cm, pH 4–7, IPG strips. Following an active rehydration 12 h step, the same IEF program applied for saturation labeling DIGE samples was performed. Second dimension was performed in the same conditions as two-dimensional DIGE experiment in 12.5% polyacrylamide gels. Fluorescence images of the gels were obtained using a Typhoon 9400 scanner at a resolution of 100ppm. Gels were subsequently poststained by a conventional silver staining and scanned using a GS-800 Calibrated Densitometer (BioRad).

MS Identification of Spots of Interest—Differential spots were identified by MS/MS using whole tissue 2-DE gels. For this purpose, preparative gels were matched with the master gel from the DIGE experiment using DeCyder and the differential spots were picked manually from the gel. Protein spots were automatically in-gel digested using the Ettan Digester (GE Healthcare). The digestion protocol used was that of Shevchenko *et al.* (10) with minor variations. The gel pieces were rinsed with 50 mM ammonium bicarbonate in 50% methanol and acetonitrile 70% and dried in a Speedvac. Modified porcine trypsin at a final concentration of 20 ng/μl in 20 mM ammonium bicarbonate was added to the dry gel pieces and the digestion proceeded at 37 °C overnight. Finally, 60% acetonitrile and 0.1% formic acid was added for peptide extraction. An aliquot of the above digestion solution was mixed with an aliquot of α-cyano-4-hydroxycinnamic acid in 30% aqueous acetonitrile, 15% 2-propanol and 0.1% trifluoroacetic acid. This mixture was deposited using the thin layer method, onto a 384 Opti-TOF 123 × 81 mm matrix-assisted laser disorption ionization (MALDI) plate (Applied Biosystems) and allowed to dry at room temperature. MALDI-MS and MS/MS data

were obtained in an automated analysis loop using a 4800 Plus MALDI TOF/TOF Analyzer (Applied Biosystems). Automated analysis of mass data was performed using the 4000 Series Explorer Software version 3.5.3 (Applied Biosystems). MALDI-MS and MS/MS data were combined through the GPS Explorer Software Version 3.6 to search a nonredundant protein database (NCBI nr 2008.06.08; 6572387 sequences, and Swissprot 56.5; 402482 sequences), without taxonomical restriction, using the Mascot software version 2.2 (Matrix Science) (11), and with the subsequent parameters: fixed modifications, carbamido methylation of cysteines; variable modifications, methionine oxidation; precursor mass tolerance = 50 ppm, fragment mass tolerance = 0.6 Da and allowing one missed cleavage. The MASCOT threshold score was fixed in each case on a correspondent *p value* = 0.05, therefore allowing less than 5% probability of incorrect identification. MALDI-MS and MS/MS spectra, and database search results were manually inspected in detail using the aforementioned software.

IHC Analysis of Altered Proteins—Among all proteins identified, six were analyzed by IHC: ferritin light chain, annexin A4, myosin regulatory light 2, smooth muscle isoform, vimentin, hemoglobin, and hsp27 (total protein and phosphorylated forms: S82 and S78). For this purpose, new OCT embedded arterial specimens were used: six ACB from transplant origin and six PRB from bypass surgery (controls). Five 100× magnification images were obtained from every IHC (supplemental Fig. S1A) to quantify positive area using the AxioVision 4.5 software (Carl Zeiss). Areas not corresponding to intima layer were first removed from each image as to quantify only positive cells from the intima (supplemental Fig. S1B). A script created with this software allowed to automatically recognize positive areas from each image and to quantify them (supplemental Fig. S1C). Whole intima area was additionally evaluated (supplemental Fig. S1D) in order to calculate the percentage of immunostained area using the subsequent equation: immunostaining % = (intimal positive area/entire intimal area in the image) × 100. Final considered immunostaining % was the mean of the five measured images.

Statistical Analysis—For the analysis by two-dimensional DIGE, a two-tailed t-Test was performed (*p value* ≤ 0.05). On the other hand, in the validation phase performed by IHC, we applied a one-tailed t-Test (*p value* ≤ 0.05). A Kolmogorov-Smirnov Test was applied to check the normal distribution of each artery type group (radial and coronary) for all validated proteins. Results obtained indicated normality of every population assayed. A PCA analysis of the DIGE experiment was performed with the differential spots from an Anova Test (*p value* ≤ 0.05) of the four groups under study.

RESULTS

Saturation Labeling DIGE Analysis and Protein Identification—The four possible combinations for protein abundance differential analysis of atherosclerotic arteries compared with control ones were assayed. Additionally, both control groups (PCN and PRB) were also compared in order to determine whether different arterial origin could introduce variations when radial artery is used as control. The Student's t-Test performed for this analysis showed no significant differences. The differential protein abundance analysis from the atherosclerotic arteries compared with control ones revealed 30 spots to be altered in total (Fig. 4*A*): six up-regulated and four down-regulated in ACB *versus* PRB, two up-regulated and nine down-regulated in ACN *versus* PCN, two down-regulated in ACB *versus* PCN, three up-regulated and 10 down-regulated in ACN *versus* PRB.

A PCA analysis was performed with the 41 spots found significantly varied within the four groups in an Anova Test (*p value* ≤ 0.05). The results confirmed an adequate grouping of the samples as can be seen in the plot (Fig. 4*B*). Moreover, control and pathological specimens were clearly separated by the first principal component.

Twenty-nine out of the 30 differential spots were identified by MS/MS on Cy3 labeled preparative gels, corresponding to 13 unique proteins (Table I). When proteins identifications were performed with nonlabeled silver-stained gels (supplemental Fig. 3) the 29 identifications reported were coincident. Seven proteins were found up-regulated, corresponding to: collagen α-1(VI) chain (2 spots), ferritin light chain (FLC), hemoglobin, hsp27, GRP78, serum amyloid protein (SaP), and SM22α (2 spots).; whereas six were down-regulated: annexin A4 (ANXA4), microfibril-associated glycoprotein 4 (MFAP4), myosin regulatory light 2, smooth muscle isoform (MRLC), osteoglycin (5 spots), transglutaminase 2 (3 spots) and vimentin (6 spots). All varied spots, in which comparison they were found, *p value* from *t* test, average ratio and the correspondent identified protein, are shown on Table I.

Validation of Protein Differential Abundance by IHC—From these altered proteins, six were selected for IHC analysis: FLC, hemoglobin, ANXA4, MRLC, vimentin, and hsp27 (total protein and phosphorylated forms: S82 and S78). Among these, three correspond to the proteins not previously reported in liquid chromatography tandem MS (LC-MS/MS) studies of human coronary intima layer (12): FLC, ANXA4, and MRLC. Colocalization of hemoglobin and FLC was also investigated. Percentage of immunostaining was calculated with AxioVision 4.5, as described above, and differential protein abundance was considered significant when Student's t-Test *p value* ≤ 0.05. Differential abundance observed by DIGE in these four proteins was confirmed by IHC, as can be observed in Figs. 5 and Fig. 6.

Ferritin Light Chain (Fig. 5A, B, C)—Student t-Test performed with the immunostaining percentages calculated with AxioVision software corroborated ferritin light chain up-regulation in atherome plaque (*p value* = $1.9 \cdot 10^{-3}$). Abundant extracellular deposits of ferritin light chain were observed in the intima from ACN samples, mainly located at the lipid core, as well as many positive macrophages/foam cells, that may have phagocytosed those deposits present in the lipid core and in the fibrous cap. In contrast, radial artery only presented occasional positive macrophages within the intima and especially in the lipid core.

Hemoglobin (Fig. 5D, E, F)—The increase of hemoglobin within atherosclerotic coronary intima observed by two-dimensional DIGE was corroborated by IHC analysis (*p value* = $5 \cdot 10^{-4}$). Hemoglobin deposits presented a similar distribution to FLC deposits within atherosclerotic coronary intima. Positive macrophages/foam cells were present in the lipid core and the fibrous cap of affected arteries,

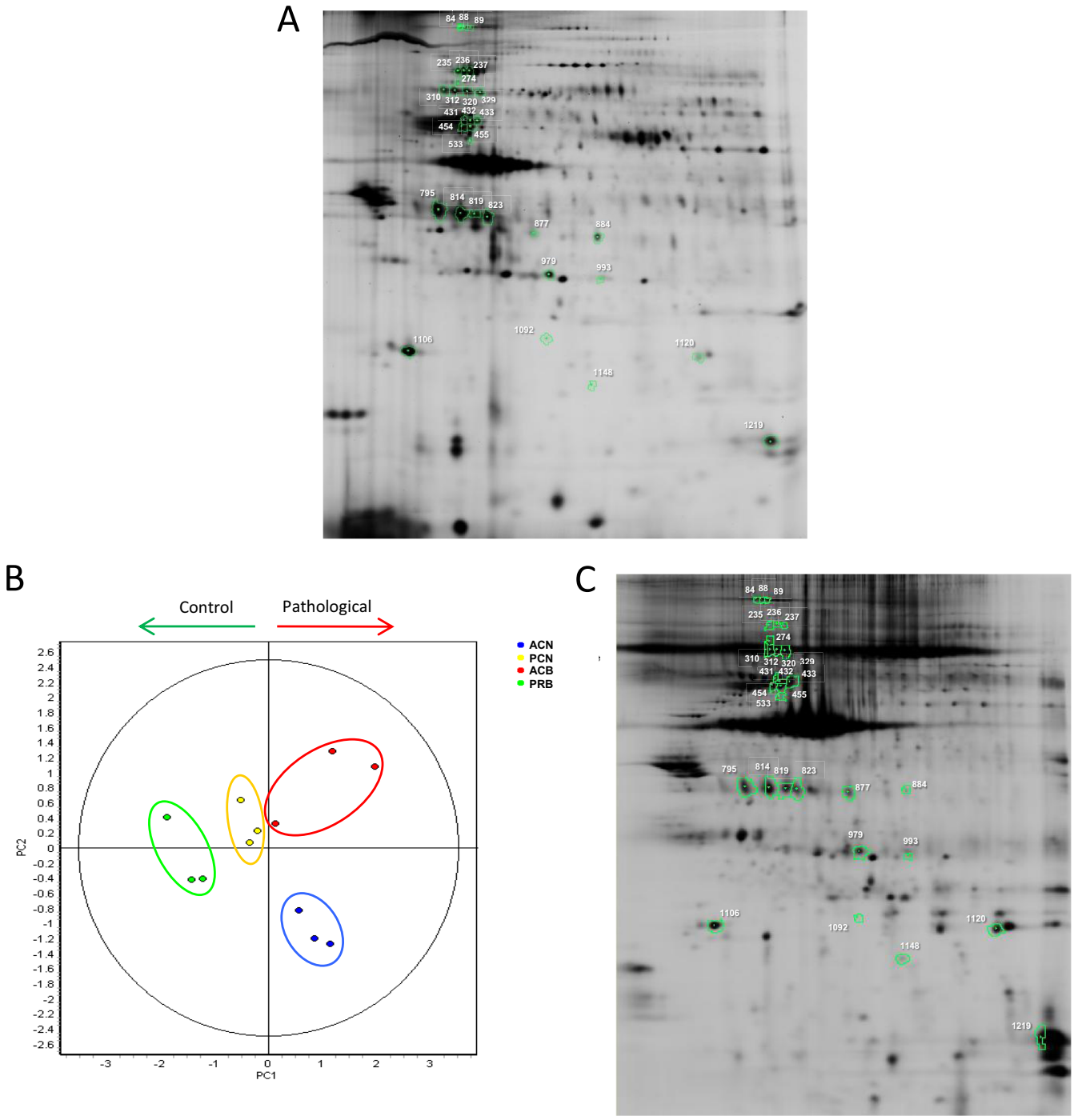

FIG. 4. **Results from the differential protein abundance analysis of atherosclerotic coronary intima.** A differential abundance analysis of the atherosclerotic coronary intima proteome was performed by saturation labeling two-dimensional-DIGE analysis. Assayed comparisons were: pathological *versus* control from the same origin (ACB *versus* PRB, ACN *versus* PCN) and pathological *versus* control from different origin (ACB *versus* PCN, ACN *versus* PRB). Comparison of control samples from different origin (PCN *versus* PRB) was also performed, but no significant results were found. Spots found significantly varied (*p value* $\leq$ 0.05) and with a fold change greater than 2.0 or lower than -2.0, are represented in a representative two-dimensional DIGE gel (*A*). In addition, principal components analysis (PCA) was performed with the spots found significantly varied in an Anova Test performed with the four groups under study (*p value* $\leq$ 0,05), where an adequate grouping of the arteries can be shown (*B*). Moreover, control and pathological samples are separated by the first principal component in the plot. The altered spots were identified on an extract of whole atherosclerotic coronary artery tissue, where correspondent proteins are noted (*C*).

TABLE I

Protein identifications of significant varied spots from DIGE analysis. Spots found significantly varied (p value ≤ 0.05) after Student's t-Test analysis of the four comparisons applied (ACB vs. PRB, ACN vs. PCN, ACB vs. PCN and ACN vs. PRB) are listed in the Table. p value from the t-Test and the average ratio are also reported, together with the details of the protein identification obtained in the correspondent spot (accession number of the protein in the searched database, unique peptides detected and sequence coverage). ACB: atherosclerotic coronary biopsy, PRB: preatherosclerotic radial biopsy, ACN: atherosclerotic coronary necropsy, PCN: preatherosclerotic coronary necropsy

Spot Num	Comparison	t-test p value	Av. Ratio	Protein identification	Accesion number (NCBInr or SwissProt)	Unique peptides detected	Sequence coverage (%)
84	ACB/PRB	0.022	3.49	————————	–	–	–
88	ACB/PRB	0.017	3.31	Collagen α-1(VI) chain	P12109	11	11
	ACN/PRB	0.0025	2.07				
89	ACB/PRB	0.049	2.47	Collagen α-1(VI) chain	P12109	5	6
235	ACN/PCN	0.0048	−3.68	Transglutaminase 2	gi 39777597	9	18
	ACN/PRB	0.044	−4.28				
236	ACN/PCN	0.048	−2.42	Transglutaminase 2	gi 39777597	9	18
237	ACN/PCN	0.0083	−2.79	Transglutaminase 2	gi 39777597	10	20
274	ACB/PRB	0.024	2.63	GRP78	gi 73968066	8	16
310	ACN/PRB	0.024	−2.59	Microfibril-associated glycoprotein 4	P55083	6	19
312	ACN/PRB	0.029	−2.72	Microfibril-associated glycoprotein 4	P55083	6	19
320	ACB/PRB	0.05	−2.81	Microfibril-associated glycoprotein 4	P55083	5	19
	ACN/PRB	0.034	−3.15				
329	ACN/PRB	0.012	−3.73	Microfibril-associated glycoprotein 4	P55083	5	19
431	ACN/PCN	0.02	−6.08	Vimentin	P08670	34	67
432	ACN/PCN	0.038	−5.87	Vimentin	P08670	31	66
433	ACN/PCN	0.024	−4.21	Vimentin	P08670	34	68
454	ACN/PCN	0.015	−2.93	Vimentin	P08670	31	68
	ACN/PRB	0.041	−4.03				
455	ACN/PCN	0.013	−2.11	Vimentin	P08670	22	45
533	ACB/PCN	0.012	−2.46	Vimentin	P08670	29	57
795	ACN/PRB	0.026	−2.24	Osteoglycin	gi 33150528	10	28
814	ACB/PRB	0.043	−3.35	Osteoglycin	gi 33150528	8	25
	ACN/PRB	0.027	−3.02				
819	ACN/PRB	0.037	−2.27	Osteoglycin	gi 33150528	12	34
823	ACB/PRB	0.023	−3.69	Osteoglycin	gi 33150528	8	33
	ACN/PRB	0.02	−3.45				
877	ACN/PCN	0.021	−3.99	Osteoglycin	gi 33150528	3	8
884	ACB/PRB	0.024	−4.2	Annexin IV	P09525	24	64
979	ACB/PRB	0.035	5.62	Serum amyloid protein	gi 576259	10	34
993	ACB/PRB	0.024	4.37	Hsp27	gi 114614145	13	63
1092	ACN/PRB	0.025	16.04	Ferririn light chain	P02792	2	14
1106	ACB/PCN	0.049	−4.9	Myosin regulatory light 2, smooth muscle isoform	gi 119936529	11	66
1120	ACN/PCN	0.0059	6.99	SM22α	Q01995	16	63
1148	ACN/PRB	0.035	4.46	SM22α	Q01995	18	71
1219	ACN/PCN	0.028	4.69	Hemoglobin	gi 999565	7	63

whereas positive macrophages were barely present in radial artery intimas.

Annexin A4 (Fig. 6A, B, C)—The down-regulation of ANXA4 observed on biopsy atherome plaques by DIGE, could be corroborated by IHC. The percentages of immunostaining were found significantly varied by a Student's t-Test (*p value* $= 1.3 \cdot 10^{-3}$). Positive cells found in both arterial intimas were mainly VSMCs. Although less abundant, some positive macrophages and ECs were observed.

Myosin Regulatory Light 2, Smooth Muscle Isoform (Fig. 6D, E, F)—A down-regulation of MRLC in the atherosclerotic coronary intima, was observed in the differential abundance analysis, and IHC assays performed were able to validate this alteration, because the Student's t-Test applied showed a significant result (*p value* $= 2.6 \cdot 10^{-5}$). Positive cells observed in the intima from atherosclerotic and control arteries were VSMCs and ECs. Positive VSMCs were present at the fibrous cap and close to the media layer, within the plaque, but not in its lipid core. In contrast, radial intimas showed abundant MRLC positive VSMCs. Positive ECs were less frequent than positive VSMCs in both arteries.

Vimentin (Fig. 6G, H, I)—Six different spots identified as vimentin were found down-regulated. Variation in the IHC% results obtained was statistically significant (*p value* $= 1.2 \cdot 10^{-6}$). Intima layer from PRB showed abundant vimentin positive VSMCs and some ECs. An important decrease in

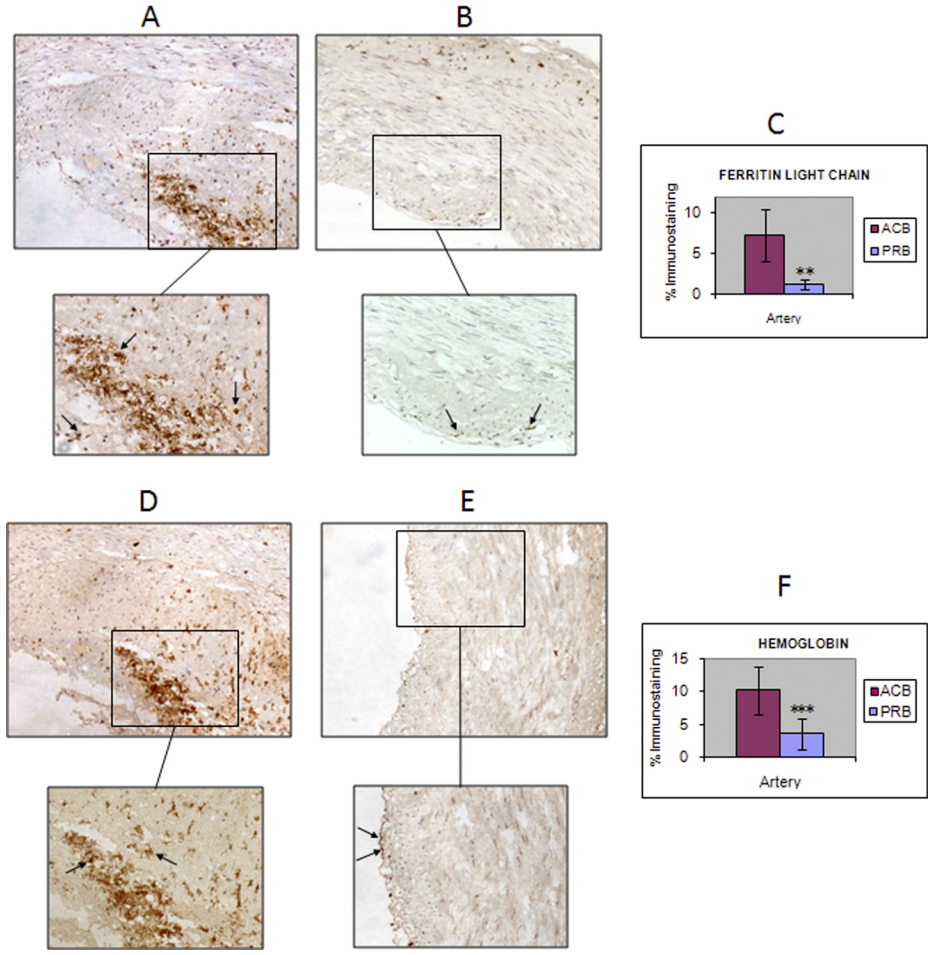

FIG. 5. **IHC results from ferritin light chain and hemoglobin point out colocalization of both proteins.** The differential abundance of FLC (*A*, atherosclerotic coronary; *B*, preatherosclerotic radial) and Hb (*D*, atherosclerotic coronary; *E*, preatherosclerotic radial) in the atherosclerotic coronary intima, observed by DIGE analysis, was validated by IHC in an independent cohort of arteries (six atherosclerotic coronaries and six radial arteries, both from biopsy origin). Mean values of immunostaining % from these assays are represented in the plot, together with the standard deviation (error bars) (*C*, FLC; *F*, Hb). Colocalization of FLC and Hb positive macrophages/foam cells and protein deposits can be observed (*A* and *D*) *Closed-end arrow*: macrophages/foam cells.

positive-VSMCs in ACN intima can be observed, within the fibrous cap.

Hsp27 (supplemental Fig. S2)—The analysis of total hsp27 protein yielded no significant differences in atherosclerotic coronary intima, although a decrease of the total protein amount can be observed when considering the whole artery tissue (supplemental Fig. S2, A, B). In addition, IHC analysis of two of the phosphorylations described for hsp27 (in Serines S82 and S78) within the atherosclerotic coronary intima also reported no significant differences (supplemental Fig. S2; S82: C, D; S78: E, F).

DISCUSSION

Proteomic studies performed to date in atherosclerosis involve plasma (13), circulating cells (particularly monocytes) (14, 15), and atherome tissue analysis (7). Proteomic analysis of atherome tissue has been mostly carried out by studying the tissue as a whole. This may be a misleading approach because of the great complexity of a sample composed by three different layers and several cell types that have different behaviors in each layer. In addition, adventitial and medial proteome may mask protein alterations occurring at the intima, where major changes during atherosclerosis initiation and development are produced. LMD constitutes a valuable tool for the isolation of the arterial layers, in order to study them separately from the others. Coronary layers were studied recently by LC-MS/MS analysis together with whole tissue proteome, which constitutes the most extensive description of coronary artery proteome appeared to date (12). However, comparative proteomic analysis of any arterial layer during atherogenesis has only been performed once, by focusing on carotid intima layer proteoglycans compared with mammary intimal ones, using a semi-quantitative approach based on peptide intensities from MS analysis (16). In previous studies (9), we isolated human coronary and aorta intima and media layers by LMD and we analyzed them by two-dimensional DIGE and LC-MS/MS. The optimum methodology developed (9) is here applied to perform the first protein differential abundance analysis of atherosclerotic coronary intima compared with preatherosclerotic arteries. Results of this analysis have pointed out altered levels of 13 proteins within the atherosclerotic coronary intima, which are implicated in the migrative capacity of VSMCs, ECM composition, coagulation, apoptosis, heat shock response, and intraplaque hemorrhage deposition.

A PCA analysis performed with all the 41 significant spots (p value ≤ 0.05) on an Anova Test showed a proper grouping of

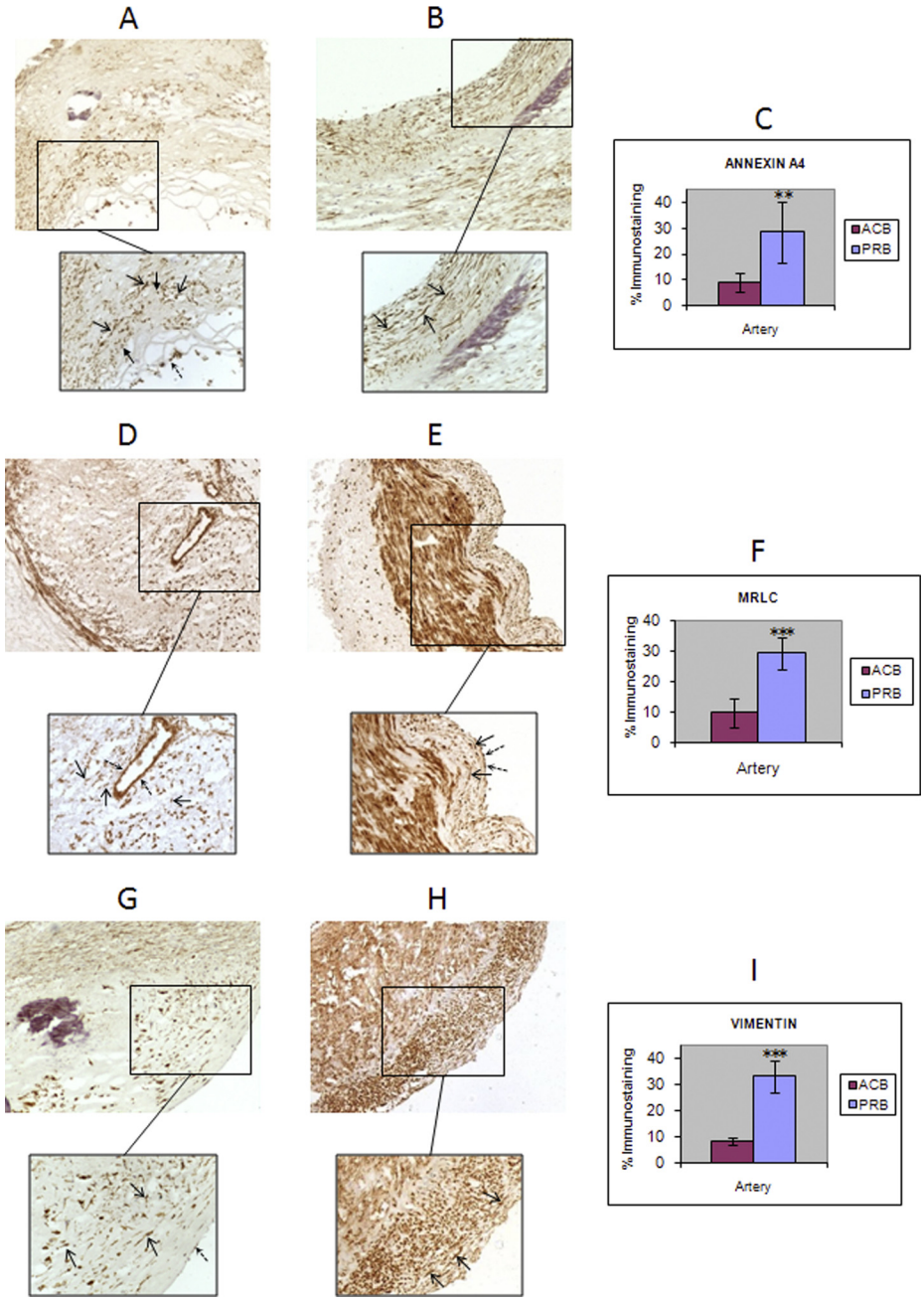

FIG. 6. **IHC results from annexin A4, MRLC and vimentin.** The differential abundance of ANXA4 (*A*, atherosclerotic coronary; *B*, preatherosclerotic radial), MRLC (*D*, atherosclerotic coronary; *E*, preatherosclerotic radial) and vimentin (*G*, atherosclerotic coronary; *H*, preatherosclerotic radial) in the atherosclerotic coronary intima, observed by DIGE analysis, was validated by IHC in an independent cohort of arteries (six atherosclerotic coronaries and six radial arteries, both from biopsy origin). Mean values of immunostaining % from these assays are represented in the plot, together with the standard deviation (error bars) (*C*, ANXA4; *F*, MRLC, *I*, vimentin). *Open-end arrow*: VSMCs. *Closed-end arrow*: macrophages/foam cells. *Discontinuous arrow*: ECs.

all the 2-DE gels in their assessed classes. In addition, first principle component clearly separated pathological samples from control ones, somehow indicating a characteristic proteomic profile of the atherosclerotic coronary intima. Concerning sample origin, in our samples we can observe that atherosclerotic coronary biopsies were not grouped with necropsy ones within the PCA plot, what implies that their proteomic content may be different. One issue to consider is the possibility of varied protein degradation levels depending on tissue origin, which could influence observed differences; particularly when they are found between necropsy and biopsy groups. In fact, the PCA graph points out that the sample source affects the proteomic profile. However, both sample types yielded good quality profiles by two-dimensional DIGE analysis and sample groups coming from different origin were successfully compared. In this sense, differential spots found while comparing necropsies and biopsies groups, *i.e.* 235, 88, 320, 454, 814, and 823, were corroborated by results observed when comparing only biopsies, which discards degradation influence on the results obtained in the necropsy-biopsy comparisons. In the same way, we were able to validate by IHC differences found either in biopsies or necropsies, using biopsy samples. On the other hand, both preatherosclerotic groups included in the study locate very close in the plot, despite their

different arterial origin, which validates them both as appropriate controls for the analysis. Moreover, differential abundance analysis comparing both groups showed no significant results following t-Test analysis (p value ≤ 0.05).

We searched for the 13 proteins found altered on the protein list from human coronary intima with hyperplasia published by Bagnato *et al.* (12). Among these proteins, ANXA4, MRLC, and ferritin LC were not identified at the intimal layer, although they were detected in the whole tissue proteome. This fact strongly supports the concept that the combination of LMD and two-dimensional DIGE is a complementary alternative to shotgun proteomics, not only because of its value for differential abundance analysis, but also for the identification of potential biomarkers in its specific location. These three proteins were validated by IHC in an independent cohort of arteries (six ACBs *versus* six PRBs), together with vimentin, one of the most varied proteins in terms of average ratio and number of isoforms altered, and Hb.

Altough protein ANXA4 is mainly expressed on epithelial tissue, IHC analysis of this protein in ACB has shown ANXA4 expression in VSMCs and macrophages within the arterial intima. Moreover, its decreased expression at the intima from ACB artery with respect to the PRB is associated with a correspondent drop off in the expression of this protein by intimal VSMCs. Annexin A5 (ANXA5) is the better known member of the annexin family and shares 97% homology with ANXA4. Both proteins have a crucial anticoagulant role in pregnancy success preventing disseminated intravascular coagulopathy (49). These findings suggest the possibility that the decrease in ANXA4 found in the atherosclerotic arterial intima may contribute to an impairment of the anticoagulation machinery, therefore increasing the risk of thrombosis. The antiapoptotic properties of ANXA5 may also be present in his homolog ANXA4. Therefore, the decreased levels of ANXA4 in VSMCs within the plaque may involve an increased risk of apoptosis, which could be of special importance in VSMCs from the fibrous cap, because apoptotic events are involved in cap thinning leading to plaque rupture (3).

MRLC is a subunit of the myosin complex from VSMCs, which regulates the contractility of these cells and thereby their migration ability. The phosphorylation of this subunit is pivotal to generate the driving force in the migration of VSMCs. MRLC dephosphorylation has been observed in VSMCs cultured in presence of aggregated LDLs as well as in intermediate coronary atherosclerotic lesions (17), which implies an inhibition of their migration and wound repair capacity. The decrease of this subunit in the atherosclerotic intima was mainly found in the IHC analysis in the lipid core, where LDL deposition may influence the migration capacity of VSMCs. Our results suggest that LDL aggregates may inhibit MRLC synthesis within VSMCs in the atherosclerotic coronary intima, somehow influencing MRLC phosphorylation process, which is crucial in the switch in the VSMCs to a migrative phenotype. Besides, the decrease in vimentin found in the atherosclerotic intima enforces this change in the migrative capacity of VSMCs. Hence, vimentin is the major constituent of the intermediate filaments of the cytoskeleton and it thereby plays a crucial role in cell contractility and migration. Preatherosclerotic intima from radial arteries presented a high proportion of MRLC- and vimentin-positive VSMCs. This may reflect its migrative state, which is consistent with their recent recruitment from media layer. The reduction in positive VSMCs within the atherosclerotic intima observed in both cases, points out a change in this cell′s phenotype, lacking of migrative properties. Moreover, positive cells in affected intimas were mainly detected at the shoulder of the lesions and in the area nearby the media layer, in contrast with a very occasional presence at the lipid core, thereby reflecting a spatial gradient in the migrative phenotype. The reduction of vimentin-positive VSMCs in the atherosclerotic intima is consistent with previous studies of IM expression in atherosclerotic plaques (18).

Ferritin is an oligomer of 24 subunits, which constitutes the major intracellular iron storage protein in all organisms (19). Two different types of subunits are assembled to form a ferritin molecule: the heavy chain (H) and the light chain (L). The proportion of each chain in the oligomer depends on the tissue and it is related with its iron binding and release capacity. The heavy chain has a more dynamic storage and release capacity than the light chain, which is prevalent in the oligomer from tissues where long-term iron storage is required. Ferritin has been several times associated with cardiovascular disease and has led to the so-called iron hypothesis, which is based in the association of elevated free circulating iron levels with an increased cardiovascular risk (19). As a result, elevated serum ferritin levels have also been associated with increased atherosclerotic progression and acute myocardial infarction (20), and peripheral artery disease risk (19). FLC was found altered in the atherosclerotic plaque in two previous proteomic studies performed with whole artery extracts (21, 22). In the one hand, FLC was associated with human carotid plaque instability (21). On the other hand, an increase of this subunit was observed in atherosclerotic coronaries (22), although its location in the tissue was not analyzed. In this study, we have corroborated an increase in FLC within atherosclerotic coronary, located at the intima, where the increase was observed to be very significant (average ratio of 16.04 in differential abundance analysis). IHC analysis showed FLC expression in extracellular protein deposits and macrophages/foam cells. Conversely, FLC expression at the media and adventitia layers was limited to occasional macrophages. An increase in the whole molecule of ferritin was previously found in foam cells within human atherosclerotic coronary and aorta (23). The toxicity of free ferric iron because of its capacity to generate free radical damage is prevented by their storage within the ferritin molecule. Our results have pointed out a huge up-regulation in the light chain of the ferritin assembly at the atherosclerotic coronary intima,

which is consistent with a need in the lesion for long-term storage ferritin molecules to prevent oxidative stress from free iron deposits. A colocalization of FLC and hemoglobin positive cells and deposits was observed following immunostaining (Fig. 5). This colocalization appears to be provoked by intraplaque hemorrhage events within the atherosclerotic lesion, recruiting erythrocytes to the plaque that contribute to the increase in hemoglobin. Moreover, the iron clearance pathway seems to activate within the plaques, resulting on an increase of FLC. These results are consistent with previous findings reporting intraplaque hemorrhage as a driving force leading to plaque vulnerability (24, 25). In addition, hemoglobin was found augmented in apoE deficient mice fed with a high fat diet and injected with *Porphyromonas gingivalis*, which developed greater atherosclerotic lesions, compared with the same mice with a correspondent fat diet but without the bacterial inoculation (26).

Among the 13 proteins found varied, some of them were previously found altered in atherosclerosis. Osteoglycin has been associated with atherosclerosis development in animal models and human coronary arteries, where *in situ* hybridization and IHC analysis were used to study its expression pattern (27, 28). We have identified osteoglycin at the atherosclerotic coronary intima and two-dimensional DIGE differential abundance analysis indicates that there is an important down-regulation of this protein with respect to preatherosclerotic arteries, which is consistent with previous findings that stated an up-regulation on coronary osteoglycin-positive VSMCs at the initiation of the lesion and a decrease on advanced plaques (28). SaP was found to be increased in atherosclerotic human aortic intima (29) and in human coronary plaques (30), where it has been shown to colocalize with apolipoproteins (30). Furthermore, elevated levels of SaP have been associated with cardiovascular risk and it has been shown to bind high density lipoproteins and very low density lipoproteins with high affinity (31). Nonetheless, its role in atherosclerosis development remains unclear. Transglutaminase 2 was found increased in preatheroslclerotic coronary artery by IHC and, with the progression of the lesion, an increase within the fibrotic tissue surrounding the plaque was indeed observed (32). Conversely, a lower expression was found in the lipid core (32). As we have studied the intima layer as a whole, the decrease observed in atherosclerotic coronary intimas may be related with a decrease in the protein level in the lipid core. These results highlight the limitation of studying the entire intima, thereby suggesting further analysis of the different regions present: lipid core, calcified nodules, fibrous cap etc., which will constitute a continuation in our purpose of delaminating the proteomic profile of the atherosclerotic coronary. Different subtypes of collagen have been detected within the atherome plaque (33). Among collagen subtypes, collagen I and III are the most abundant species in the atherosclerotic lesion, although collagen IV, V (33), and VI (34) have also been observed to be up-regulated in the plaque. In our study the chain α-1 from collagen VI was found increased in the atherosclerotic coronary intima thereby corroborating previous findings (34). On the other hand, there was another ECM protein found altered in the atherosclerotic coronary intima: MFAP4. This glycoprotein participates in cellular adhesion, and his down-regulation in the intima of the atherosclerotic coronary may come from an instability of the cell-ECM interactions. Moreover, MFAP4 has been associated with vascular pathology because of its location in a chromosomic region linked to increased intracranial aneurism risk (35). SM22α has been also found altered in the differential abundance analysis. This protein is considered a marker of a contractile phenotype of VSMCs. Its implication in atherosclerosis development has been proved using murine models (36, 37) and human atherosclerotic coronaries (28). These studies demonstrate that a decrease in the protein in VSMCs is pivotal in the phenotypical change of contractile VSMCs in the media to a proliferative state at the intima and therefore in the lesion development. In the other hand, studies of medial layer calcification in peripheral arteries (named Mönckeberg sclerosis) have pointed out an increase of SM22α in VSMCs from calcified regions (38), thereby suggesting a similar role of the protein in vascular calcification occurred during atherosclerosis. The up-regulation of SM22α in the affected coronary intima may come from an increase of the protein in a subset of VSMCs from calcified regions of the plaque, which would have shift the balance of total protein amount, because VSMCs from the preatherosclerotic intima, that should be in a proliferative state do not express the protein, and calcification events in such specimens are not expected. Finally, two heat shock proteins were found up-regulated in the atherosclerotic coronary intimas: hsp27 and GRP78. Concerning hsp27, our previous studies performed with atherosclerotic carotid tissue, secretome and plasma have proven a down-regulation of the total protein amount in carotid stenosis patients (39), as well as a decrease of the most abundant phosphorylated isoform (phosphorylation of Serine S82) in the atherosclerotic carotids (40). The increase observed in the present study in the spot identified as hsp27 indicates that one of the several isoforms of this protein (41) is augmented in the atherosclerotic coronary intima. IHC analysis of total hsp27 showed no significant differences in atherosclerotic coronary intima, although a decrease of the total protein amount can be observed when considering the whole artery tissue (supplemental Fig. S2, A, B), which corroborates previous findings. Moreover, IHC analysis of two of the phosphorylations described for hsp27 (in Serines S82 and S78) within the atherosclerotic coronary intima also reported no significant differences (supplemental Fig. S2; S82: C, D; S78: E, F). Attending to the spot intensity, this isoform is indeed minority, and may not affect the total protein amount balance. A more exhaustive study of the different hsp27 isoforms present in the coronary intima would be necessary to asses which isoform is increased and its possible role in

atherosclerosis development. GRP78 is a member of the hsp70 family specifically expressed in the endoplasmic reticulum. The expression of the proteins from Hsp70 family has been observed to be induced in several inflammatory processes (42) and may have cytoprotective capacity in atherosclerotic tissues (43). The increase of this protein is consistent with the relatively recent hypothesis that has defined atherosclerosis as an inflammatory disease (1, 2). In addition, previous studies of our group found hsp70 increased in circulating monocytes during ACS (14). Specifically, GRP78 has been found increased in several studies of experimental atherosclerosis (44–47), and has been observed to negatively regulate the procoagulant activity of the tissue factor via functional inhibition and directly binding to it (48).

In conclusion, our proteomic focus within the atherosclerotic coronary intima performed by LMD coupled with two-dimensional DIGE has shown the alteration of 13 proteins implicated in the migrative capacity of VSMCs, ECM composition, coagulation, apoptosis and heat shock response, and intraplaque hemorrhage deposition. The proteins validated by IHC: ferritin LC, ANXAA4, MRLC, vimentin, and Hb may be potential novel tissue biomarkers of atherosclerosis, although further analysis in a greater group of patients is needed to assess their predictive value. The approach here described is oriented to the discovery of tissue biomarkers, which are pivotal to better understand the pathology, but has the limitation that their diagnostic potential relies on the possibility that they are released to blood in a sufficient amount to be detected, which needs to be proved in successive studies.

Acknowledgments—We would like to thank Gemma Barroso, Dr. Veronica Moral and Ana Isabel Carrasco, from Proteomic Unit, Hospital Nacional de Paraplejicos, SESCAM, Toledo, Spain, for their dedication and support with protein identifications, Montse Martinez, from Proteomic Unit, UCM, Parque Cientifico, Madrid, for her help with DeCyder software, and Dr. Miguel Rivera's group, from the Hospital la Fe, Valencia, for transplant samples collection.

* This work was supported by grants from the *Ministerio de Educación y Ciencia* (BFU-2005-08838), CAM (Proteomarkers S2006/GEN-0247), the *Instituto de Salud Carlos III* (FIS PI070537, FIS PI080970), and *Mutua Madrileña Automovilista* (20174/004). Fernando de la Cuesta and Gloria Alvarez-Llamas were supported by FIS (Refs: FI06/00583, CP09/00229). We have declared no conflicts of interest.

[S] This article contains supplemental material.

‡‡ To whom correspondence should be addressed: Department of Immunology, IIS-Fundacion Jimenez Diaz. Avda. Reyes Catolicos 2, 28040 - Madrid (Spain). Fax: (+34) 915448246; E-mail: fvivanco@fjd.es.

§§ Both authors contributed equally to this work.

REFERENCES

1. Libby, P. (2002) Inflammation in atherosclerosis. *Nature* **420,** 868–874
2. Ross, R. (1999) Atherosclerosis–an inflammatory disease. *N. Engl. J. Med.* **340,** 115–126
3. Dzau, V. J., Braun-Dullaeus, R. C., and Sedding, D. G. (2002) Vascular proliferation and atherosclerosis: new perspectives and therapeutic strategies. *Nat. Med.* **8,** 1249–1256
4. Fuster, V., Fayad, Z. A., and Badimon, J. J. (1999) Acute coronary syndromes: biology. *Lancet* **353 Suppl 2,** S115–S119
5. Virmani, R., Kolodgie, F. D., Burke, A. P., Farb, A., and Schwartz, S. M. (2000) Lessons from sudden coronary death: a comprehensive morphological classification scheme for atherosclerotic lesions. *Arterioscler. Thromb. Vasc. Biol.* **20,** 1262–1275
6. Libby, P., and Aikawa, M. (2002) Stabilization of atherosclerotic plaques: new mechanisms and clinical targets. *Nat. Med.* **8,** 1257–1262
7. de la Cuesta, F., Alvarez-Llamas, G., Gil-Dones, F., Martin-Rojas, T., Zubiri, I., Pastor, C., Barderas, M. G., and Vivanco, F. (2009) Tissue proteomics in atherosclerosis: elucidating the molecular mechanisms of cardiovascular diseases. *Expert. Rev. Proteomics* **6,** 395–409
8. Wilson, K. E., Marouga, R., Prime, J. E., Pashby, D. P., Orange, P. R., Crosier, S., Keith, A. B., Lathe, R., Mullins, J., Estibeiro, P., Bergling, H., Hawkins, E., and Morris, C. M. (2005) Comparative proteomic analysis using samples obtained with laser microdissection and saturation dye labelling. *Proteomics* **5,** 3851–3858
9. de la Cuesta, F., Alvarez-Llamas, G., Maroto, A. S., Donado, A., Juarez-Tosina, R., Rodriguez-Padial, L., Pinto, A. G., Barderas, M. G., and Vivanco, F. (2009) An optimum method designed for two-dimensional DIGE analysis of human arterial intima and media layers isolated by laser microdissection. *Proteomics Clin. Appl.* **3,** 1174–1184
10. Shevchenko, A., Wilm, M., Vorm, O., and Mann, M. (1996) Mass spectrometric sequencing of proteins silver-stained polyacrylamide gels. *Anal. Chem.* **68,** 850–858
11. Perkins, D. N., Pappin, D. J., Creasy, D. M., and Cottrell, J. S. (1999) Probability-based protein identification by searching sequence databases using mass spectrometry data. *Electrophoresis* **20,** 3551–3567
12. Bagnato, C., Thumar, J., Mayya, V., Hwang, S. I., Zebroski, H., Claffey, K. P., Haudenschild, C., Eng, J. K., Lundgren, D. H., and Han, D. K. (2007) Proteomics analysis of human coronary atherosclerotic plaque: a feasibility study of direct tissue proteomics by liquid chromatography and tandem mass spectrometry. *Mol. Cell. Proteomics* **6,** 1088–1102
13. Vivanco, F., Padial, L. R., Darde, V. M., de, la, Cuesta, F., Alvarez-Llamas, G., Diaz-Prieto, N., and Barderas, M. G. (2008) Proteomic Biomarkers of Atherosclerosis. *Biomark. Insights.* **3,** 101–113
14. Barderas, M. G., Tuñón, J., Dardé, V. M., de la Cuesta, F., Durán, M. C., Jiménez-Nácher, J. J., Tarín, N., López-Bescós, L., Egido, J., and Vivanco, F. (2007) Circulating human monocytes in the acute coronary syndrome express a characteristic proteomic profile. *J. Proteome. Res.* **6,** 876–886
15. Barderas, M. G., Tuñón, J., Dardé, V. M., de la Cuesta, F., Jiménez-Nácher, J. J., Tarín, N., López-Bescós, L., Egido, J., and Vivanco, F. (2009) Atorvastatin modifies the protein profile of circulating human monocytes after an acute coronary syndrome. *Proteomics* **9,** 1982–1993
16. Talusan, P., Bedri, S., Yang, S., Kattapuram, T., Silva, N., Roughley, P. J., and Stone, J. R. (2005) Analysis of intimal proteoglycans in atherosclerosis-prone and atherosclerosis-resistant human arteries by mass spectrometry. *Mol. Cell. Proteomics* **4,** 1350–1357
17. Padro, T., Pena, E., Garcia-Arguinzonis, M., Llorente-Cortes, V., and Badimon, L. (2008) Low-density lipoproteins impair migration of human coronary vascular smooth muscle cells and induce changes in the proteomic profile of myosin light chain. *Cardiovasc. Res.* **77,** 211–220
18. Osborn, M., Caselitz, J., Püschel, K., and Weber, K. (1987) Intermediate filament expression in human vascular smooth muscle and in arteriosclerotic plaques. *Virchows Arch. A Pathol. Anat. Histopathol.* **411,** 449–458
19. You, S. A., and Wang, Q. (2005) Ferritin in atherosclerosis. *Clin. Chim. Acta* **357,** 1–16
20. Sullivan, J. L. (2009) Iron in arterial plaque: modifiable risk factor for atherosclerosis. *Biochim. Biophys. Acta* **1790,** 718–723
21. Lepedda, A. J., Cigliano, A., Cherchi, G. M., Spirito, R., Maggioni, M., Carta, F., Turrini, F., Edelstein, C., Scanu, A. M., and Formato, M. (2009) A proteomic approach to differentiate histologically classified stable and unstable plaques from human carotid arteries. *Atherosclerosis* **203,** 112–118
22. You, S. A., Archacki, S. R., Angheloiu, G., Moravec, C. S., Rao, S., Kinter, M., Topol, E. J., and Wang, Q. (2003) Proteomic approach to coronary atherosclerosis shows ferritin light chain as a significant marker: evidence consistent with iron hypothesis in atherosclerosis. *Physiol. Genomics* **13,** 25–30

23. Yuan, X. M. (1999) Apoptotic macrophage-derived foam cells of human atheromas are rich in iron and ferritin, suggesting iron-catalysed reactions to be involved in apoptosis. *Free Radic. Res.* **30,** 221–231
24. Yamagishi, S., Ueda, S., Matsui, T., Nakamura, K., Imaizumi, T., Takeuchi, M., and Okuda, S. (2007) Pigment epithelium-derived factor (PEDF) prevents advanced glycation end products (AGEs)-elicited endothelial nitric oxide synthase (eNOS) reduction through its anti-oxidative properties. *Protein Pept. Lett.* **14,** 832–835
25. Kolodgie, F. D., Gold, H. K., Burke, A. P., Fowler, D. R., Kruth, H. S., Weber, D. K., Farb, A., Guerrero, L. J., Hayase, M., Kutys, R., Narula, J., Finn, A. V., and Virmani, R. (2003) Intraplaque hemorrhage and progression of coronary atheroma. *N. Engl. J. Med.* **349,** 2316–2325
26. Madan, M., and Amar, S. (2008) Toll-like receptor-2 mediates diet and/or pathogen associated atherosclerosis: proteomic findings. *PLoS One* **3,** e3204
27. Fernández, B., Kampmann, A., Pipp, F., Zimmermann, R., and Schaper, W. (2003) Osteoglycin expression and localization in rabbit tissues and atherosclerotic plaques. *Mol. Cell. Biochem.* **246,** 3–11
28. Shanahan, C. M., Cary, N. R., Osbourn, J. K., and Weissberg, P. L. (1997) Identification of osteoglycin as a component of the vascular matrix. Differential expression by vascular smooth muscle cells during neointima formation and in atherosclerotic plaques. *Arterioscler. Thromb. Vasc. Biol.* **17,** 2437–2447
29. Li, X. A., Hatanaka, K., Ishibashi-Ueda, H., Yutani, C., and Yamamoto, A. (1995) Characterization of serum amyloid P component from human aortic atherosclerotic lesions. *Arterioscler. Thromb. Vasc. Biol.* **15,** 252–257
30. Stewart, C. R., Haw, A., 3rd, Lopez, R., McDonald, T. O., Callaghan, J. M., McConville, M. J., Moore, K. J., Howlett, G. J., and O'Brien, K. D. (2007) Serum amyloid P colocalizes with apolipoproteins in human atheroma: functional implications. *J. Lipid Res.* **48,** 2162–2171
31. Li, X. A., Yutani, C., and Shimokado, K. (1998) Serum amyloid P component associates with high density lipoprotein as well as very low density lipoprotein but not with low density lipoprotein. *Biochem. Biophys Res. Commun.* **244,** 249–252
32. Cho, B. R., Kim, M. K., Suh, D. H., Hahn, J. H., Lee, B. G., Choi, Y. C., Kwon, T. J., Kim, S. Y., and Kim, D. J. (2008) Increased tissue transglutaminase expression in human atherosclerotic coronary arteries. *Coron. Artery Dis.* **19,** 459–468
33. Katsuda, S., Okada, Y., Minamoto, T., Oda, Y., Matsui, Y., and Nakanishi, I. (1992) Collagens in human atherosclerosis. Immunohistochemical analysis using collagen type-specific antibodies. *Arterioscler. Thromb.* **12,** 494–502
34. Kittelberger, R., Davis, P. F., and Stehbens, W. E. (1990) Type VI collagen in experimental atherosclerosis. *Experientia* **46,** 264–267
35. Yamada, S., Utsunomiya, M., Inoue, K., Nozaki, K., Inoue, S., Takenaka, K., Hashimoto, N., and Koizumi, A. (2004) Genome-wide scan for Japanese familial intracranial aneurysms: linkage to several chromosomal regions. *Circulation* **110,** 3727–3733
36. Feil, S., Hofmann, F., and Feil, R. (2004) SM22alpha modulates vascular smooth muscle cell phenotype during atherogenesis. *Circ. Res.* **94,** 863–865
37. Wamhoff, B. R., Hoofnagle, M. H., Burns, A., Sinha, S., McDonald, O. G., and Owens, G. K. (2004) A G/C element mediates repression of the SM22alpha promoter within phenotypically modulated smooth muscle cells in experimental atherosclerosis. *Circ. Res.* **95,** 981–988
38. Shanahan, C. M., Cary, N. R., Salisbury, J. R., Proudfoot, D., Weissberg, P. L., and Edmonds, M. E. (1999) Medial localization of mineralization-regulating proteins in association with Monckeberg's sclerosis: evidence for smooth muscle cell-mediated vascular calcification. *Circulation* **100,** 2168–2176
39. Martin-Ventura, J. L., Duran, M. C., Blanco-Colio, L. M., Meilhac, O., Leclercq, A., Michel, J. B., Jensen, O. N., Hernandez-Merida, S., Tuñón, J., Vivanco, F., and Egido, J. (2004) Identification by a differential proteomic approach of heat shock protein 27 as a potential marker of atherosclerosis. *Circulation* **110,** 2216–2219
40. Park, H. K., Park, E. C., Bae, S. W., Park, M. Y., Kim, S. W., Yoo, H. S., Tudev, M., Ko, Y. H., Choi, Y. H., Kim, S., Kim, D. I., Kim, Y. W., Lee, B. B., Yoon, J. B., and Park, J. E. (2006) Expression of heat shock protein 27 in human atherosclerotic plaques and increased plasma level of heat shock protein 27 in patients with acute coronary syndrome. *Circulation* **114,** 886–893
41. Scheler, C., Müller, E. C., Stahl, J., Müller-Werdan, U., Salnikow, J., and Jungblut, P. (1997) Identification and characterization of heat shock protein 27 protein species in human myocardial two-dimensional electrophoresis patterns. *Electrophoresis* **18,** 2823–2831
42. Jacquier-Sarlin, M. R., Fuller, K., Dinh-Xuan, A. T., Richard, M. J., and Polla, B. S. (1994) Protective effects of hsp70 in inflammation. *Experientia* **50,** 1031–1038
43. Bielecka-Dabrowa, A., Barylski, M., Mikhailidis, D. P., Rysz, J., and Banach, M. (2009) HSP 70 and atherosclerosis–protector or activator? *Expert. Opin. Ther. Targets* **13,** 307–317
44. Feaver, R. E., Hastings, N. E., Pryor, A., and Blackman, B. R. (2008) GRP78 upregulation by atheroprone shear stress via p38-, alpha2beta1-dependent mechanism in endothelial cells. *Arterioscler. Thromb. Vasc. Biol.* **28,** 1534–1541
45. Dickhout, J. G., Hossain, G. S., Pozza, L. M., Zhou, J., Lhoták, S., and Austin, R. C. (2005) Peroxynitrite causes endoplasmic reticulum stress and apoptosis in human vascular endothelium: implications in atherogenesis. *Arterioscler. Thromb. Vasc. Biol.* **25,** 2623–2629
46. Pedruzzi, E., Guichard, C., Ollivier, V., Driss, F., Fay, M., Prunet, C., Marie, J. C., Pouzet, C., Samadi, M., Elbim, C., O'dowd, Y., Bens, M., Vandewalle, A., Gougerot-Pocidalo, M. A., Lizard, G., and Ogier-Denis, E. (2004) NAD(P)H oxidase Nox-4 mediates 7-ketocholesterol-induced endoplasmic reticulum stress and apoptosis in human aortic smooth muscle cells. *Mol. Cell. Biol.* **24,** 10703–10717
47. Zhou, J., Werstuck, G. H., Lhoták, S., de Koning, A. B., Sood, S. K., Hossain, G. S., Møller, J., Ritskes-Hoitinga, M., Falk, E., Dayal, S., Lentz, S. R., and Austin, R. C. (2004) Association of multiple cellular stress pathways with accelerated atherosclerosis in hyperhomocysteinemic apolipoprotein E-deficient mice. *Circulation* **110,** 207–213
48. Bhattacharjee, G., Ahamed, J., Pedersen, B., El-Sheikh, A., Mackman, N., Ruf, W., Liu, C., and Edgington, T. S. (2005) Regulation of tissue factor–mediated initiation of the coagulation cascade by cell surface grp78. *Arterioscler. Thromb. Vasc. Biol.* **25,** 1737–1743
49. Masuda, J., Takayama, E., Satoh, A., Ida, M., Shinohara, T., Kojima-Aikawa, K., Ohsuzu, F., Nakanishi, K., Kuroda, K., Murakami, M., Suzuki, K., Matsumoto, I. (2004) Levels of annexin IV and V in the plasma of pregnant postpartum women. *Thromb Haemost* **91,** 1129–1136